IAC-18,C4,7-C3.5,5,x46021

The SpaceDrive Project - Thrust Balance Development and New Measurements of the Mach-Effect and EMDrive Thrusters

Matthias Kößling [a], Maxime Monette [b], Marcel Weikert [c] and Martin Tajmar [d]*

[a] Institute of Aerospace Engineering, Technische Universität Dresden, Marschnerstrasse 32, 01307 Dresden, Germany, matthias.koessling@tu-dresden.de
[b] Institute of Aerospace Engineering, Technische Universität Dresden, Marschnerstrasse 32, 01307 Dresden, Germany, maxime.monette@tu-dresden.de
[c] Institute of Aerospace Engineering, Technische Universität Dresden, Marschnerstrasse 32, 01307 Dresden, Germany, marcel.weikert@tu-dresden.de
[d] Institute of Aerospace Engineering, Technische Universität Dresden, Marschnerstrasse 32, 01307 Dresden, Germany, martin.tajmar@tu-dresden.de
* Corresponding Author

Abstract

Forces claimed by potential propellantless propulsion systems like the Mach-Effect thruster or the EMDrive are in the µN or even sub-µN range. In this paper, an automated thrust balance design capable of measuring forces of 100 nN for thrusters with a maximum mass of 10 kg is described to test these claims. The torsion balance features an electromagnetic calibration method, adjustable magnetic damping and tilt control as well as electromagnetic shielding. All onboard electronics can be controlled wirelessly via an infrared module for serial communication. Power is supplied to the balance using three separate liquid metal feedthroughs: one for voltages up to 500 V and frequencies up to 200 kHz, one for high voltage up to 30 kV DC or AC, and one for high frequency signals up to 3 GHz. The thruster can be rotated by 180° to measure three different thrust directions without breaking the vacuum and changing the setup in order to gain confidence and refute e.g. thermal drifts. The whole balance is controlled via a script language implemented in LabVIEW. We tested Mach-Effect thrusters provided by Woodward and our own built model exploring higher frequencies and mixed-signals that are believed to create significantly higher thrusters. Also a magnetostrictive version was built and tested. For the EMDrive, several different frequencies and setups (with/without dielectric insert, flat/spherical end caps) were tested. So far, only thermal drifts and no real thrust has been observed in all our measurements.

Keywords: Breakthrough Propulsion, Propellantless Propulsion, EMDrive, Mach-Effect-Thruster, Thrust Balance

Nomenclature

a	-	Acceleration [m/s^2]
c	-	Speed of Light [m/s]
E_0	-	Energy Density [Jm^3/kg]
F	-	Force [N]
G	-	Gravitational Constant [Nm^2/kg^2]
k	-	Spring Stiffness [Nm/°]
K	-	Calibration Factor [N/m]
m	-	Mass [kg]
ω	-	Angular Frequency [Hz]
ρ_0	-	Material Density [kg/m^3]
t	-	Time [s]

Abbreviations

AC	-	Alternating Current
DC	-	Direct Current
HDPE	-	High Density Polyethylene
HV	-	High Voltage
IR	-	Infrared
MET	-	Mach-Effect-Thruster
RF	-	Radio Frequency
SNR	-	Signal-to-Noise-Ratio
VNA	-	Vector-Network-Analyzer

1. Introduction

Forces claimed in peer-reviewed publications to be generated by thrusters without the expense of propellant and with a superior efficiency to that of the photon rocket not only would revolutionize the concept of interstellar travel, but also challenge fundamental principles of physics. Although different theories provide an explanation for forces that can be generated by devices such as the EMDrive [1],[2] or the Mach-Effect-Thruster [3],[4], there is a large step between the measurement of a torsion balance beam displacement and the confirmation of propellantless, unidirectional thrust. Our SpaceDrive Project at TU Dresden aims to develop cutting-edge thrust balances to thoroughly investigate these claims [5],[6]. The device described here is an automated, low-thrust torsion balance that can support a thruster weight of up to 10 kg and measures minuscule beam displacements using a laser interferometer.

In this paper, we will present our progress in testing the two most prominent claims for propellantless thrust, namely the Mach-Effect-Thruster and the EMDrive.

2. Thrust Balance

2.1. Introduction

Torsion balances are used to precisely measure the minute thrust of electric propulsion thrusters, which makes them well suited to measure the forces claimed in the Mach-Effect thruster and the EMDrive experiments. The claimed forces for these thrusters are sub-µN up to 2µN for the former [3],[4] and up to 90µN for the latter [2] depending on the power to the thrusters. Thus, if any thrust signal is to be distinguished from noise, a desirable Signal-to-Noise-Ratio (SNR) of 10 would require a measurement resolution of at least 200nN.

To help achieving this low resolution, our measurements are divided in 5 distinct sectors (Figure 1). Sector 1 represents the test segment before the power to the thruster is turned on. In sector 2, the power is quickly turned on (lasts 1s). Sector 3 is when the power to the thruster is kept on. In Sector 4, the power is quickly turned off (lasts 1s), and sector 5 is the segment after the power is turned off. This consistency allows us to take an average of many individual measurement profiles to minimize the effect of ambient noise.

The following experiments were all performed in vacuum at a pressure of 10^{-2} mbar.

2.2. Features

The displacement of the balance is measured using a laser interferometer IDS3010 by attocube with a M12/F40 sensor head. The resolution of the sensor is 1 pm, the noise is 1 nm at room temperature and approaches the resolution at 4 K.

The spring is implemented using two E-20 pivots by C-Flex with a torsional spring rate of k = 3.344 mN·m/°. These bearings support the balance beam, are mounted at the top and bottom of its central rotation axis, and allow a limited but near-frictionless rotation. The bottom pivot does not only act as a radial bearing, but also as an axial bearing; its maximal axial load is 35 kg. The 25 kg shear load resistance of the E-20 bearing is also a limiting factor. Weight imbalance at the opposing ends of the beam leads to great shear forces on the pivots. According to the current design, this imbalance should not exceed 3.0 kg, indicating the need for a counterweight on the opposite side of the experiment. In previous designs, the pivots were also used to communicate DC power to the experiment on the balance beam: one pivot was used as positive terminal and the other one as ground. However, it was promptly discovered that resistive heating in the bearing changed its spring stiffness.

To circumvent this problem, four coax liquid contacts were installed on the balance (Figure 2). The contacts are placed in the rotation axis of the beam to distribute power to the balance while minimizing friction in rotation. Galinstan, a metal alloy that becomes liquid at -18 °C, was purchased from Geratherm Medical AG and is used as the liquid connection. Figure 2 shows a cross-section of one liquid contact. The center wire is normally positive while the surrounding copper shell is grounded.

The calibration of the balance is done with a voice-coil LA05-05-000A by BEI Kimco. The permanent magnet is mounted onto the beam and the solenoid is fixed to a 3-axes translation stage MVT 40B-D15-XYZ-SK by OWIS. A current flowing through the solenoid generates a magnetic field that repels or attracts the magnet. The voice-coil was calibrated using an analytical balance M-Pact AX224 by Sartorius, and a Keithley 2450 is used for precise current control and measurement.

Since the preload on the pivot influences the overall spring stiffness of the balance, and because the voice-coil has only a limited linear range, the relative position of the solenoid to the voice-coil should stay within a certain range. Therefore, a rotation stepper motor DMT 100-D53-HSM-v6 by OWIS is installed at the bottom of the balance's central axis that can apply a torque to the bottom bearing and change the zero position of the balance before the start of an experiment. Two TCST 2103 light barriers are then used to validate the position of the voice-coil.

A permanent magnet damps the oscillation of the balance using eddy-currents (Figure 3). It consists of two neodymium magnets (⌀50mm x 1.2mm, 1.2T) positioned inside a U-shaped steel (1.0503) bracket mounted on the beam of the balance. The 90mm x 55mm x 2mm copper plate is mounted on a sledge that can be moved up or down by a Stögra motor SM56-1-18JL1V Z138 to vary the damping factor. The motor is controlled using a circuit board from Weeder Technologies (WTMCD-M), and a relay is used to turn it off if not in use.

The frame of the balance consists of four layers. The first layer is made from aluminum profiles and rests on the guiding rails of the vacuum chamber. The second layer rests on top of the first one, and is composed of vibration-damping sorbothane to damp the low frequencies from the surrounding environment. The next layer is another layer of aluminum profiles. The last layer is a frame on which the torsion balance and all its components are mounted. It is connected to the previous layer with three threaded M8 pins that can be adjusted to level the balance. Two of these pins are connected to stepper motors SM56-1-18JL1V Z138, allowing to vary the tilt of the balance by 4° in the short direction and 6° in the long direction of the balance. The motors are controlled by two WTMCD-M circuit boards from Weeder Technologies and can be disconnected via two relays.

All major parts of the balance (experiment/thruster box, electronics box and balance arm) are encapsulated with 0.5 mm plates

made from mu-metal with a very high magnetic permeability to reduce the electromagnetic interaction between the inside and the outside. A Stögra stepper motor SM56-1-18JL1V is used to rotate the box, enabling the measurement of different thruster orientations without breaking vacuum. Again, the motor is controlled by a WTMCD-M circuit board and is turned off through a relay when not in use.

On the other side of the beam, a similar box is installed and contains the main electronics of the balance and experiments. The two most important ones are an infrared (IR) module IrDA-To-PC by Mikroelektronika for contactless communication and a LabJack T7 which has several analog inputs and outputs, thermocouples and digital pins. The main voltage for the balance is 28 VDC with a maximum current of 9 A. DC-DC converters provide other voltage levels for the IR device and the LabJack.

Some experiments to be performed on the balance require high voltage (HV). One way to provide this voltage is to put the supply on the balance, in the electronics box, but the power is limited by the size of the box. To feed HV and high power to the balance, a HV liquid contact is installed above the four low-voltage liquid contacts. It is designed for 30 kV DC or AC. Like in the other coax contacts, the center pin is at a high potential and is submerged in Galinstan while a surrounding ring, also filled with Galinstan, acts as the shield. Between the two liquid metal baths, a U-shaped cross-section prevents any direct path from the high to the low potential to prevent arcing (Figure 4). The HV contact can only be used in high vacuum to prevent arcing.

In previous tests, it was shown that the amplifier for the EMDrive draws a significant amount of DC current during its operation and subsequently heats up [6]. Duif showed a promising solution to put the amplifier outside the chamber, and built a contactless radio-frequency (RF) feedthrough for a torsion balance [7]. Since this feedthrough is too bulky and does not fit in our vacuum chamber, a new design was necessary (Figure 5). The feedthrough consists of two N-type connectors, each equipped with a soldering pin. These central pins are both placed in a container filled with Galinstan, while the connector's outer shield is connected via a separate Galinstan-filled container. A reflection power loss of 4 dB was directly measured over this RF feedthrough, which still leaves enough power for the EMDrive inside the chamber with the amplifier outside without the need to worry about how to cool the amplifier or to limit the length of thrust profiles. It was observed that additional RF components and the positioning of the EMDrive and the RF cables significantly influenced reflection losses in the system which still needs to be optimized.

2.3. Characterization

2.3.1. Drift Removal

The thrust balance and the laser interferometer have an inherent drift. Additionally, a part of the power that is transmitted to the thruster is converted into thermal energy and heats up the thruster, leading to thermal drift. These drifts can be compensated using different methods. The inherent drift of the balance and the interferometer are constant during the whole measurement and can be removed with a linear fit that is calculated from the displacement measurement before the power is turned on (Sector 1). Figure 6 shows how this method is used for a measurement with inherent and thermal drifts. In Figure 6b, this fit is removed, such that Sector 1 follows a constant line, the thermal drift in other sectors is still visible. The second method can remove the inherent drift, and the thermal drift to some extent. To achieve this, the fit for the inherent drift is again calculated for Sector 1, followed by another fit for Sector 5, where the power is turned off. Lastly, the last point of the first fit is connected with the first point of the second fit using a straight line (Figure 6c). In Figure 6d, these lines are again removed from the whole measurement. In this example, the resulting signal is a slightly noisy but clearly constant measurement, which is not always the case, since the thermal drift is mostly non-linear (for both heating up and cooling down). Our software implemented a non-linear fit only to describe cooling down as in this case no thrust shall be produced.

2.3.2. Noise

The noise of the thrust balance can vary a bit between measurements because of sources of perturbation in the lab, such as vacuum pumps. A sample noise is shown in Figure 7, containing the average of 140 profiles resulting in a standard deviation of 11 nN. This means that a reasonable SNR of >100 is expected if a thrust of 2 μN is to be measured.

2.3.3. Damping

As already mentioned, the damping mechanism of the balance relies on eddy-currents. The current setting of the copper plate between the magnets results in a damping ratio of 0.43 (Figure 8). The damping was calculated using the logarithmic decrement [8]. The balance damping lies close to the recommended range of 0.5-0.8 for damping [9].

2.3.4. Calibration

A calibration is performed before and after each measurement. The calibration consists of measuring the balance response to a steady pulse of seven different force values, to be applied by a separately calibrated voice-coil (-12, -8, -4, 0, 4, 8 and 12 μN) (Figure 9a). The average of the balance displacement

is plotted against the commanded force to calculate the force-conversion factor K. This factor is 6.7 µN/µm for the calibration shown (Figure 9b). 200 measurements of 1 µN pulses with a duration of 60 s was performed over night to ensure the accuracy of the calibration (Figure 9c). The measurements show a force of 0.9 µN, indicating a 10% discrepancy which still needs to be optimized (long term drift). Since the thruster in the MET experiment is only driven with 25 s pulses, a more representative calibration of 80 profiles with 1µN pulses and a duration of 25 s was performed (Figure 9d). The pulse duration is too short for the balance to reach steady state and the force at the end is only 0.8 µN. These measurements show that the balance can measure steady forces with 10% error for a pulse duration of 60 s. If the pulse duration falls below 30 s, the balance is too slow to measure the force exactly but an impulse-like behavior with 80% accuracy can still be detected within a few seconds.

3. Mach-Effect-Thruster

3.1. Introduction

The Mach-Effect-Thruster (MET) is a device invented by Woodward aimed to produce unidirectional thrust without the use of propellant [3]. According to Woodward's theory, a mass fluctuation can be induced in a pre-stressed, multi-layered piezoelectric stack actuator by relying on the inverse piezoelectric effect to change the mechanical energy of the device given by

$$\delta m(t) = \frac{1}{4\pi G c^2 \rho_0} \frac{\partial^2 E_0}{\partial t^2} \qquad \text{Eq. 1}$$

Based on Newton's mechanics, the mass fluctuation is converted to a net thrust when coupled to an acceleration acting on the fluctuating mass at the same frequency [3],[10]

$$F = \frac{\omega}{2\pi} \int_0^{\frac{2\pi}{\omega}} \delta m(t) a(t) \qquad \text{Eq. 2}$$

In Woodward's experiment, a sinusoidal voltage signal is applied to the piezoelectric actuator, and the required acceleration is provided by the electrostrictive properties of the material that generates a mechanical response based on the square of the applied electric field [11]. Woodward claims to have measured a thrust of 1-5 µN on a torsion balance with a sinusoidal signal and a voltage amplitude between 200-250V with even larger On-Off transients [4]. Buldrini replicated the experiment reporting a smaller measured force of 0.2 µN at a lower voltage amplitude of 100 V [12]. An alternative to the single sinusoidal voltage signal would be to apply a mixed signal composed of a signal with excitation frequency ω to which a second signal with frequency 2ω is superimposed. With this method, the acceleration required to produce the thrust is five orders of magnitude greater than the electrostrictive response when comparing the piezoelectric and electrostrictive coupling constants. Therefore, according to Woodward's theory, this method should produce much greater thrust.

Woodward is using a Carvin DCM 1000 audio amplifier with a limited frequency range as well as a step-up transformer. We previously tested the MET using a dedicated high-frequency amplifier without the need of a step-up transformer to get to high voltages. In addition, our setup allows to track the resonance frequency during testing. First tests indicated no measureable thrust in our setup with voltages up to 75 V amplitude at 31 kHz resonance frequency [6]. Here we present new measurements again with a thruster supplied by Woodward including a transformer in our setup as well as testing mixed-signals that shall generate higher thrusts. In addition, our own MET was built and tested.

3.2. Experimental Setup

The setup consists of a power circuit, the thruster and the data-acquisition system with control logic to automate the measurements. The power circuit is composed of two power supplies PS5200-04 by Elektro-Automatik, and a 200 W power amplifier based on the PA04 (APEX). The maximum voltage of one single amplifier is limited to around 90 V. Two of the amplifiers can be connected in bridge mode to double the output voltage. A RIGOL signal generator DSG2011Z is used to supply the single and mixed signals to the amplifier at the specified frequency. The voltage and the current (measured with a hall sensor) are both read using a digital oscilloscope BS-10 by Bitscope. These devices are located outside the vacuum chamber and can be controlled by a computer (Figure 10). There are also three infrared temperatures sensors GY-906 that measure the temperature of the PZT stack, the aluminum end cap and the copper block. Lastly, the output of the amplifier is applied to the thruster through a vacuum chamber feedthrough and one coaxial liquid contact.

Our own MET follows the same design as Woodward's [10] with the following differences:

- PZT disks (PIC181 from PI Ceramic) with an outer diameter of 20 mm (=1 mm larger),
- silver epoxy 8330S by MG Chemicals was used to provide better electrical contact between piezo-disks, curing time and temperature of 2h and 70°C respectively,
- only four M3x30 screws were used for pre-stressing the stack at 15MPa,
- thermally conductive epoxy 8329TCS by MG Chemicals was used to protect the stack from humidity and improve heat distribution, curing time and temperature of 1h and 80°C respectively,

These features account for the slight differences in the Q-factor, resonant and anti-resonant frequencies between the unloaded impedance spectra of the Woodward thruster and our self-built thruster, compared in Figure 12. A LabVIEW program is used to pinpoint the stack's mechanical resonance where the maximal vibration amplitude is expected by tracking the frequency with 50 Hz steps for maximum current at the commanded voltage.

3.3. Results & Discussion

The results presented in this section represent an average of 140 overnight runs for different thruster orientations, equivalently experiment box orientations (0° = forward, 90° = parallel to beam, 180° = reverse).

Thermal drift is removed from the individual profiles following the procedure described in a previous section. The first set of diagrams are force measurements for the Woodward MET, mounted via a polyethylene piece to an aluminum mounting pad on the balance. All measurements were done at the mechanical resonance frequency of 31 kHz. Figure 13 shows the averaged profiles using the amplifier in single-mode and an additional 4:1 turn-ratio transformer JA4635-AL by Coilcraft right after the amplifier to boost the voltage in the thruster in order to better resemble Woodward's original setup. Although the 0° measurement shows a peak force of 2μN at 140 V, its shape does not show impulse-like behavior. The fact that the reverse measurement (180°) does not show the same force magnitude indicates that the observed force signal most likely results from non-linear thermal drift.

We then tested the mixed-signal with the amplifier in single-mode without the transformer. The input voltage in this case was only 37 V as the maximum voltage in the mixed signal doubles as the two different signals add up. Figure 14 shows only a small signal that flips in orientation between 0° and 180° but is also more or less present in the 90° orientation, although with more noise. This also indicates that there was no real thrust present. Most importantly, according to Woodward's theory we should have expected an increase in thrust by orders of magnitude which we did not see.

For the last set of measurements with Woodward's thruster, the device was mounted on a 250 g copper block that acts as a heat sink (Figure 11). This block was then fixed to a PEEK plate, used to electrically isolate the thruster from the balance, inside the experiment box. This time, two amplifiers were used in bridge mode to boost the voltage amplitude to 180 V. As shown in Figure 15, no thrust is now observed in this configuration at the 0° direction.

We then tested our own-built MET thruster (TUD MET). Figure 16 shows no force below 100 nN for the thruster powered up to 180 V at it's mechanical resonance frequency of 36 kHz using the amplifiers in bridge-mode. The thruster was also powered at its second resonance frequency (72 kHz) without any noticeable thrust within our resolution of 100 nN as shown in Figure 17. According to Woodward's theory, thrust should have increased proportional to ω^4.

3.4. Conclusion

Given the careful precautions to eliminate the electromagnetic interactions between the devices and cables on the balance and the support structure, it is safe to assume that the small force signals observed so far most likely results from non-linear thermal drifts during the power signal. Moreover, no impulse-like behavior, observed by Woodward et al. on their balance, has been observed from either the single sinusoidal or the mixed sinusoidal signals in this experiment. The next steps of this research include building a second MET with features as close as possible to Woodward's original device, testing different vibration modes (including anti-resonance), and using a similar electronics set-up as Woodward, with an audio amplifier (DCM1000, Carvin) and a matching transformer (6:1 turn ratio, ferrite core) to employ the exact same driving conditions.

4. Magnetostrictor

4.1. Introduction

The striking similarity between the Woodward MET design and an ultrasonic transducer has led to the purchase of a magnetostrictive transducer CU18A by Etrema Products, Inc. for experiments (Figure 18). The cross-section of the transducer shows all the important elements of a MET, notably the vibrating end mass, the pre-stressed actuator, and a flexural spring [13]. This transducer can be driven with a voltage amplitude of up to 100 V and a frequency of 30 kHz, limited by eddy current losses, as specified by the data sheet, and the external mass screwed onto the output boss changes the resonance frequency and vibration amplitude. In this design, the actuation or mechanical force is provided by a solid rod of sintered Terfenol-D, a material with giant magnetostrictive strain which undergoes mechanical deformation induced by a magnetic field. The frequency sweep in Figure 19 shows the frequency response of the transducer current, at a fixed voltage, for no external mass and with a 38 g external mass. The advantage of this transducer over the MET design is its larger vibrational amplitude, which should produce larger thrust according to the mass fluctuation equation from Woodward, its availability as an off-the-shelf product and its relatively low hysteresis losses. The magnetostrictive actuator is also more robust than the MET since the spectrum shown in Figure 19 did not vary at all through the experimental runs. Lastly,

it is simply observed from the spectrum that more power can be input to the magnetostrictive transducer (higher current for the same voltage). Needless to say, that a larger effect is expected from this device on the balance. The transducer from Etrema should, however, be driven by a mixed signal, with one signal at frequency ω to which a second signal with frequency 2ω is superposed, since there is no appreciable electrostriction in the literature for this material.

4.2. Experimental Setup

The experimental setup is the same as for the MET experiment. A mass of 38 g was attached to the transducer with the recommended 13.6 Nm torque, and the transducer itself was attached to the copper block in the experiment box of the balance.

4.3. Results & Discussion

The force measurements were also performed with the transducer oriented in different directions (0° = forward, 90° = parallel to beam, 180° = reverse), and the diagrams presented in this section also show an average of 140 overnight runs. The device was first tested with a single signal, and Figure 20 seem to show on-off transients of about 0.3 µN, but although the orientation of the device is reversed in the second diagram, the measured force is not reversed. This test indicated that the electromagnetic shielding of the experiment box is imperfect, and that the greater current in the magnetostrictive transducer compared to the MET is responsible for the minute force. Measurements of the beam vibration with our laser interferometer with a high sampling frequency, with the transducer end mass oscillating with a 2 kN dynamic force, do not show beam oscillation greater than 10 nm amplitude. Temperature measurements of the external mass do not show a significant increase in the temperature. The results of the mixed signal for the magnetostrictive device do not show any signal in sector 3, when the thermal drift is removed (Figure 21). This signal has a lower voltage, so the current is also reduced.

To examine the electromagnetic influence of the sinusoidal voltage signal, a resistor was placed on the copper plate instead of the transducer (Figure 22). The resistance was 26 Ohm to get the same current for the 75 V that were applied to the transducer. The result is similar to the original measurement. Therefore, all thrust signals from the magnetostrictor were due to interactions of the electric current and no real thrusts.

4.4. Conclusion

The magnetostrictive transducer which should function in a similar way as the MET, with lower frequency but greater vibrational amplitude, did not show the any thrust. This seems to indicate that the theory developed by Woodward does not apply to this device.

5. EMDrive

5.1. Introduction

The EMDrive is another potential propellantless thruster, invented by Shawyer [1], which consists in a closed, truncated cavity in which electromagnetic waves of the microwave regime resonate in a particular mode to produce unidirectional thrust. The physical explanation behind this mechanism is highly controversial and speculative ranging from false measurements due to interaction with the Earth's magnetic field [6],[14] to new concepts [2],[15],[16].

Beside the inventor himself, experiments were carried out most notably by NASA Eagleworks Laboratories [2],[17],[18], by the Chinese Northwestern Polytechnical University [19] and our group [6],[20]. Our work initially tried to closely follow the work from White et al [2] in terms of geometry, setup and operational frequencies. First measurements indicated false thrusts due to an interaction of the large currents driving the amplifier on the balance [6]. Our new setup puts the amplifier outside the vacuum chamber due to our RF liquid metal feedthrough on the balance. Moreover, we can now electromagnetically shield the complete thruster using mu-metal sheets. The tests presented here were done for NASA's geometry including a dielectric disc as in their original setup. In addition, we also removed the disc, implemented spherical end caps and tested at higher frequencies as recommended by Shawyer.

5.2. Experimental Setup

The experiments used a manually pressed, 1.5mm thick, conical copper frustum with dimensions as close as possible to NASA's truncated cone [2]. The dielectric disc was implemented in the flat end-caps version and consisted of a 4cm-thick HDPE disk (NASA originally used 5.4cm) glued to the small end cap. Power was generated and transmitted through a system of coaxial radio-frequency (RF) components. An ANRITSU MS46121B Vector Network Analyzer (VNA) and a Seeed Studio RF Explorer 3G Spectrum Analyzer were used to examine the spectrum of the cavity itself (unloaded), identify the resonance modes, and tune the antenna to a particular resonance frequency. An electro-smog meter and a microwave leakage detector were used to examine the radiation under different setup conditions.

The EMDrive test setup shown in Figure 23 consists mainly of commercial off-the-shelf RF components. A RIGOL DSG830 frequency generator produces a signal in the range of 9kHz to 3GHz with a power level of -110dBm to 13dBm. The frequency generator is coupled to an EmPower 1164

RF amplifier with SMA coaxial cables. The amplifier has a measured amplification of 47 dB and can output up to 50 W in a frequency range of 800 MHz to 3 GHz. A MECA circulator redirects the power reflected from the vacuum chamber feedthrough to a 30dB-attenuator and then a Mini-circuits ZX47-40LN+ power meter. The circulator also protects the amplifier from reflected power in the system. These components are located outside the vacuum chamber to reduce the influence of transient currents and amplifier heating on the balance measurement.

The power is then transmitted through the vacuum chamber using a Hositrad SMA 50Ω coaxial feedthrough. To deliver the RF power from the fixed part of the system to the thrust balance, the RF feedthrough described in Section 2.2 is used.

On the thrust balance, the coaxial RF cables deliver power to a bi-directional coupler from Mini-circuits ZGBDC35-93HP. Two more power meters can measure the RF power coming from the feedthrough to the cavity as well as the power reflected from the cavity. A Maury Microwave three-stub tuner matches the 50Ω-coaxial-components to the emitter-antenna inside the copper cavity. The three-stub tuner, power meters and EMDrive are all enclosed by the mu-metal shielding of the experiment box.

In order to achieve high power in the cavity and minimize the power reflected back to the RF system, the power is delivered at a resonance frequency of the cavity, as measured with the VNA before implementing the cavity in the test setup.

Our LabView software is automatically tracking the resonance frequency to maximize the power delivered to the cavity. Resonance frequency shifts, which originate from thermal expansion of the cavity, lead to an increase in the reflected power which can be detected by the power meters. The control software tracks the maximum power input to power reflected ratio by varying the signal frequency to ensure that the cavity is driven at resonance during the whole test segment.

5.3. Results & Discussion

Figure 25a shows first experiments for the cavity including the HDPE insert at a frequency of 1933 MHz. The power shown is the power delivered into the cavity based on our power meter measurements. An average of 55 profiles with a 60s pulse shows an average force of 3.4 µN when the drift of sector 1 is removed. However, the shape of the graph seems to indicate the effect of a thermal drift rather than a net thrust coming from the cavity. The power and thrust is similar to the values reported by March (4.7 µN for 3.2 W) [18], however in their signals a step response of the torsion balance is seen and in our measurement a thermal drift of similar magnitude.

Without the HDPE disk, the measurement at an average frequency of 1920 MHz shows what seems to be thermal drift (Figure 25b) too. Here the delivered power is larger and hence the beam displacement too, which would be also consistent with a thermal effect.

The last measurement is performed at 2576 MHz with spherical end-caps and without any HDPE. Once again, a force of 3.0 µN was measured and is identified as thermal drift since it does not show the impulse-like behavior observed in 1 µN voice-coil tests (Figure 25c).

In our measurements, the power delivered to the cavity itself was smaller than the commanded power due to losses on the RF components that depended significantly on the positioning of the RF cables and shielding components in the system. This behavior can be explained by capacitive effects in the multiple connections present in the RF network. We need to further optimize our setup in order to optimize this behavior.

5.4. Conclusion

Our latest measurements on the EMDrive in different configurations and frequency ranges seem to indicate only thermal drifts. Our setup still needs to be further optimized in order to reliably quantify the power delivered to the cavity in this new configuration. Moreover, thrust measurements in different directions are still missing. To avoid the influence of superimposed reflected waves in the RF-system mounted on the balance, which sometimes leads to erratic power readings, a further circulator will be used. This circulator will be placed between the bi-directional-coupler and the balance's RF feedthrough, and will redirect the reflected power from the cavity to an attenuator and a termination.

Measurements need to be repeated with higher power level and a better understanding of the power readings.

6. Conclusion

An automated thrust balance with several liquid metal contacts and a resolution down to 11 nN was presented. Tests were done with Mach-Effect thrusters as well as with different configurations of the EMDrive. For the first time, higher frequencies and mixed-signals could be tested with the MET as well as different mounting options such as a heat sink below the thruster. In addition to Woodward's thruster model, we built our own model and tested an alternative using magnetostriction instead of piezo actuators. No thrusts were seen on any of these configurations. For the EMDrive, our setup was modified allowing the amplifier to be placed outside the vacuum chamber which allows higher power and longer thrust pulses. First tests with and without a dielectric disc as well as flat and spherical end caps

were performed and indicate thermal drifts instead of real thrusts. This needs to be further investigated.

In our next steps, we will try to more closely replicate Woodward's original MET setup and further optimize our EMDrive setup for future measurements.

Acknowledgements

We gratefully acknowledge the support for SpaceDrive by the German National Space Agency DLR (Deutsches Zentrum fuer Luft- und Raumfahrttechnik) by funding from the Federal Ministry of Economic Affairs and Energy (BMWi) by approval from German Parliament (50RS1704). We would also like to acknowledge the support from J. Heisig, J. Woodward and H. Fearn for their contributions to the ongoing experiments.

References

[1] Shawyer, R., "Second Generation EmDrive Propulsion Applied to SSTO Launcher and Interstellar Probe," *Acta Astronautica*, vol. 116, 2015, pp. 166–174. doi:10.1016/j.actaastro.2015.07.002

[2] White, H., March, P., Lawrence, J., Vera, J., Sylvester, A., Brady, D., and Bailey, P., "Measurement of Impulsive Thrust from a Closed Radio-Frequency Cavity in Vacuum," *Journal of Propulsion and Power*, vol. 33, Jul. 2017, pp. 830–841. doi:10.2514/1.B36120

[3] Woodward, J. F., *Making Starships and Stargates*, New York, NY: Springer New York, 2013. doi:10.1007/978-1-4614-5623-0

[4] Fearn, H., Rossum, N. van, Wanser, K., and Woodward, J. F., "Theory of a Mach Effect Thruster II," *Journal of Modern Physics*, vol. 06, 2015, pp. 1868–1880. doi:10.4236/jmp.2015.613192

[5] Tajmar, M., Kößling, M., Weikert, M., and Monette, M., "The SpaceDrive Project – Developing Revolutionary Propulsion at TU Dresden," *International Astronautical Congress*, 2017, p. IAC-17,C4,7-C3.5,10,x38595.

[6] Tajmar, M., Weikert, M., and Monette, M., "The SpaceDrive Project – First Results on EMDrive and Mach-Effect Thrusters," *Proceedings of the Space Propulsion Conference*, Sevilla: 2018, p. SP2018_016.

[7] Duif, C. P., "An Improved Method to Measure Microwave Induced Impulsive Forces with a Torsion Balance or Weighing Scale," *Technical Report*, 2017doi:10.13140/RG.2.2.13679.64163

[8] Soni, J., and Roy, S., "Design and Characterization of a Nano-Newton Resolution Thrust Stand," *Review of Scientific Instruments*, vol. 84, 2013doi:10.1063/1.4819252

[9] Polk, J. E., Pancotti, A., Haag, T., King, S., Walker, M., Blakely, J., and Ziemer, J. K., "Recommended Practices in Thrust Measurements," *33rd International Electric Propulsion Conference*, 2013, p. IEPC-2013-440.

[10] Tajmar, M., "Mach-Effect Thruster Model," *Acta Astronautica*, vol. 141, Dec. 2017, pp. 8–16. doi:10.1016/j.actaastro.2017.09.021

[11] Uchino, K., "Introduction to Piezoelectric Actuators and Transducers," *5th International Conference on Intelligent Materials*, 2003, p. ARO-44924.1-EG-CF.

[12] Buldrini, N., "Verification of the Thrust Signature of a Mach Effect Device," *Proceedings of the Estes Park Advanced Propulsion Workshop*, H. Fearn and L. Williams, eds., Mojave, CA: Space Studies Institute Press, 2017, pp. 83–88.

[13] Karunanidhi, S., and Singaperumal, M., "Design, Analysis and Simulation of Magnetostrictive Actuator and Its Application to High Dynamic Servo Valve," *Sensors and Actuators, A: Physical*, vol. 157, 2010, pp. 185–197. doi:10.1016/j.sna.2009.11.014

[14] Li, A. Y., and Li, S. A., "An Experiment About Parallel Circuit And The Lorentz Forces On Wires" Available: http://arxiv.org/abs/1510.07752

[15] Mcculloch, M. E., "Can the Emdrive Be Explained by Quantised Inertia?," *Progress in Physics*, vol. 11, 2015, pp. 78–80.

[16] Grahn, P., Annila, A., and Kolehmainen, E., "On the Exhaust of Electromagnetic Drive," *AIP Advances*, vol. 6, Jun. 2016, p. 065205. doi:10.1063/1.4953807

[17] Brady, D., White, H., March, P., Lawrence, J., and Davies, F., "Anomalous Thrust Production from an RF Test Device Measured on a Low-Thrust Torsion Pendulum," *50th AIAA/ASME/SAE/ASEE Joint Propulsion Conference*, Reston, Virginia: American Institute of Aeronautics and Astronautics, 2014, p. AIAA 2014-4029. doi:10.2514/6.2014-4029

[18] March, P., "Experiments with RF Cavity Thrusters," *Estes Park Advanced Propulsion Workshop*, H. Fearn and L. Williams, eds., Mojave, CA: Space Studies Institute, Inc., 2016, pp. 39–66.

[19] Juan, Y., Wang, L. I. U. X., Luo, Y. T. M., and Ning, L. J. I. N. Y., "Thrust Measurement of an Independent Microwave Thruster Propulsion Device with Three-Wire Torsion Pendulum Thrust Measurement System," vol. 37, 2016, pp. 362–371. doi:10.13675/j.cnki.tjjs.2016.02.022

[20] Tajmar, M., and Fiedler, G., "Direct Thrust Measurements of an EMDrive and Evaluation of Possible Side-Effects," *51st AIAA/SAE/ASEE Joint Propulsion Conference*, 2015, p. AIAA 2015-4083. doi:10.2514/6.2015-4083

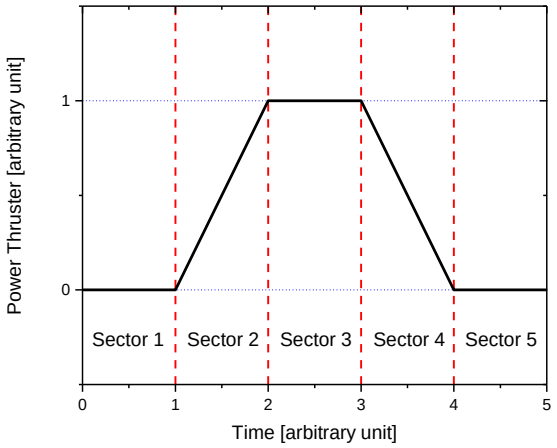

Figure 1: Sectors in Measurement

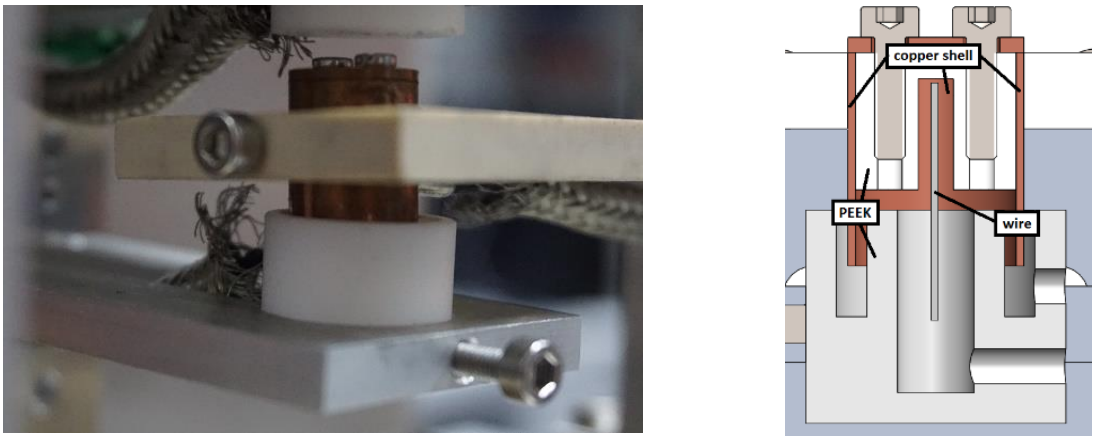

Figure 2: Coax Liquid Contact (left), Cross-Section (right)

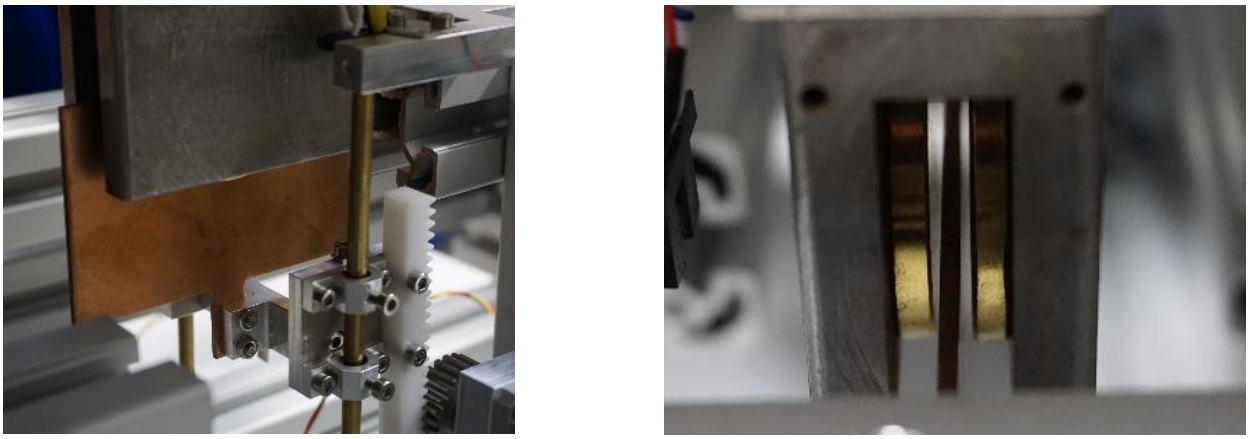

a) b)

Figure 3: Magnetic Damping Complete Setup (left), Detailed View of Plate between Magnets (right)

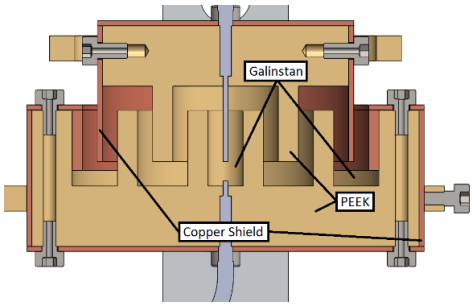

Figure 4: HV Feedthrough, cross-section

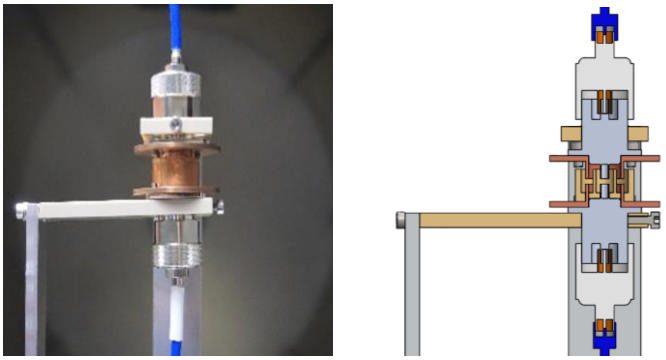

Figure 5: RF Feedthrough Complete Setup (left), Cross-Section (right)

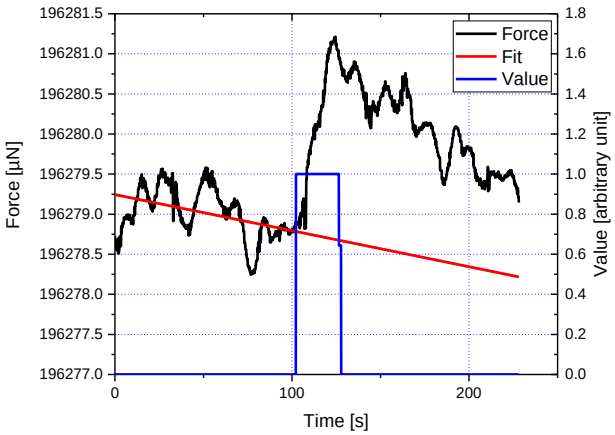

a) Methode 1, Raw Data + Fitting

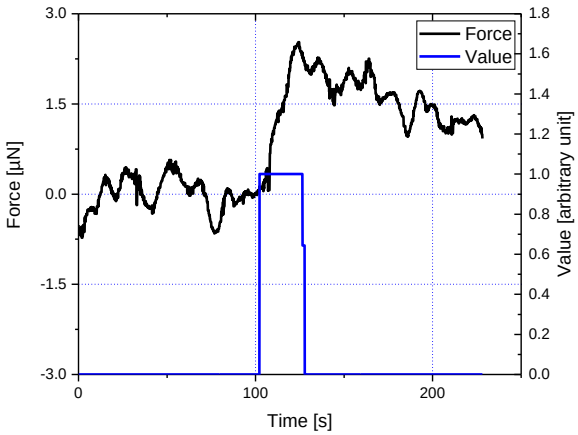

b) Methode 1, Drift Sector 1 removed

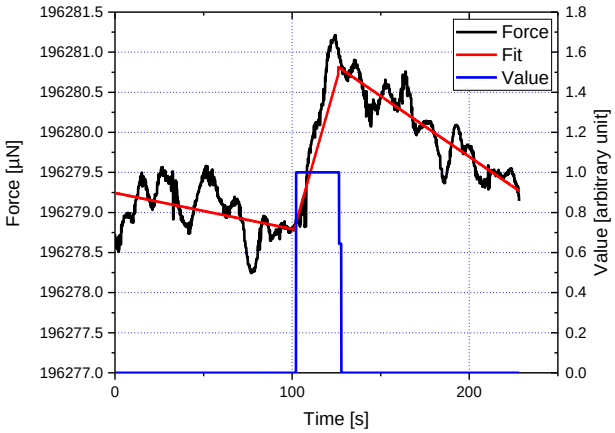

c) Methode 2, Raw Data + Fitting

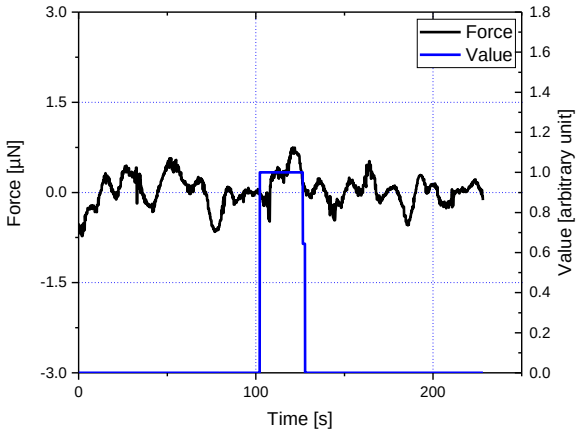

d) Methode 2, Thermal Drift removed

Figure 6: Methode 1 + 2 Drift Removal

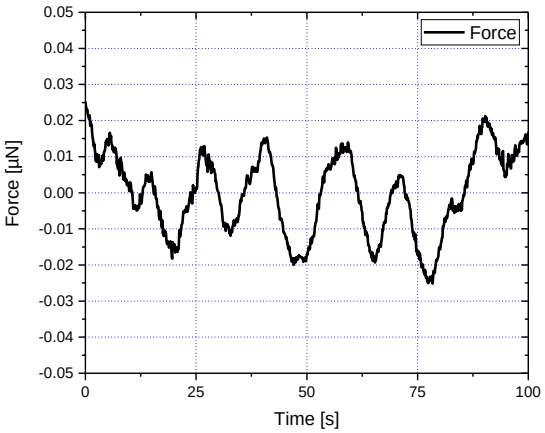

Figure 7: Sample noise measurement from 140 averaged profiles, σ = 0.011 µN

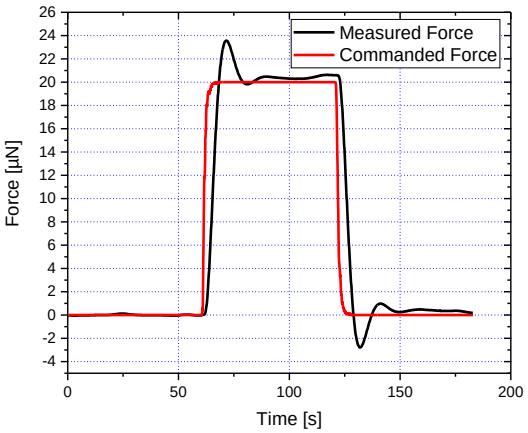

Figure 8: Damping for a force of 20 µN

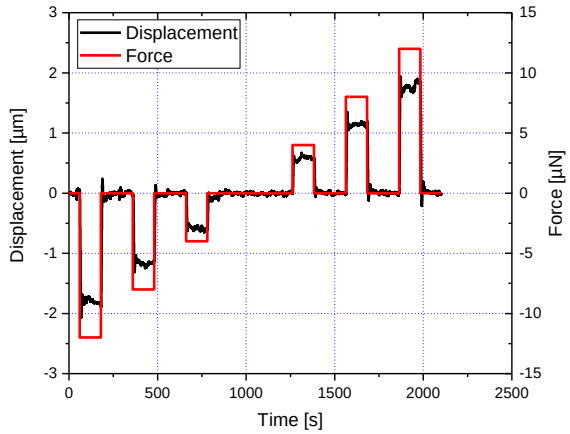

a) Calibration Run (7 Steps)

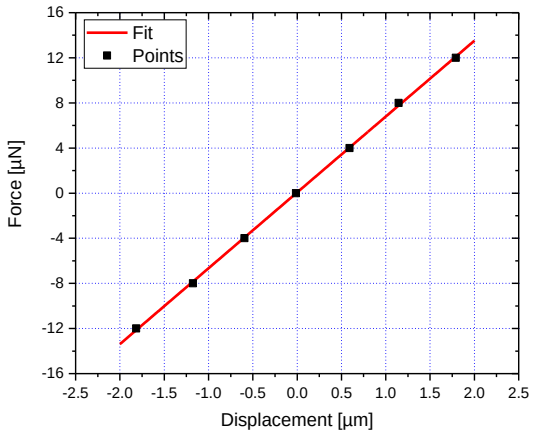

b) Average of Individual Displacements

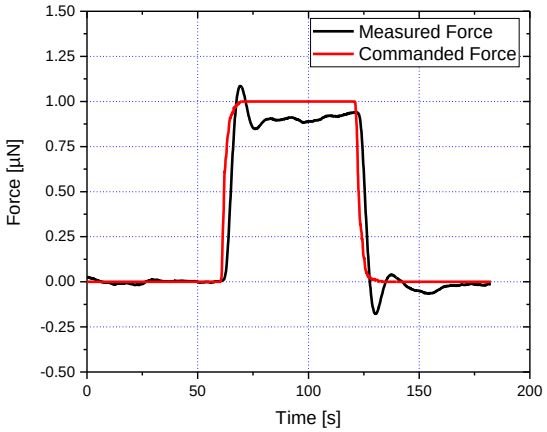

c) Average of 200 Profiles, 1 µN for 60 s

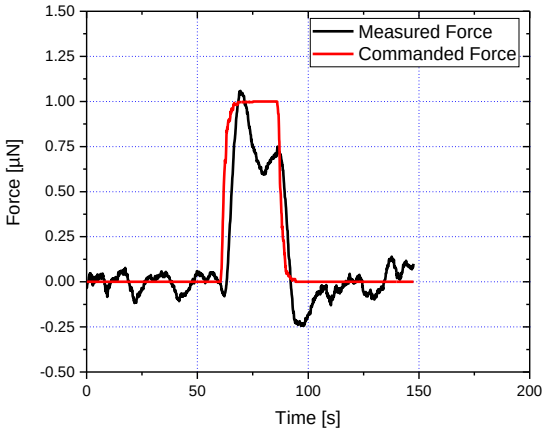

d) Average of 80 Profiles, 1 µN for 25 s

Figure 9: Voice-Coil Calibration

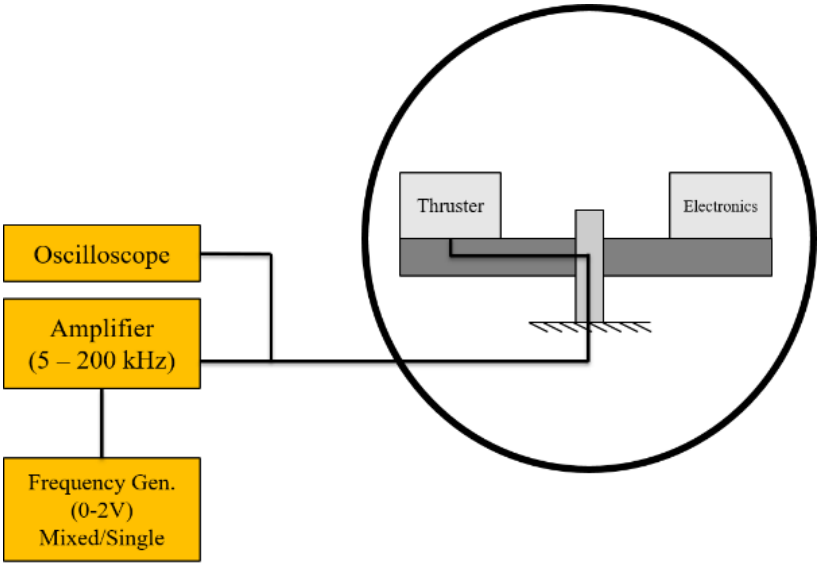

Figure 10: Mach Effect Thruster Electrical Setup

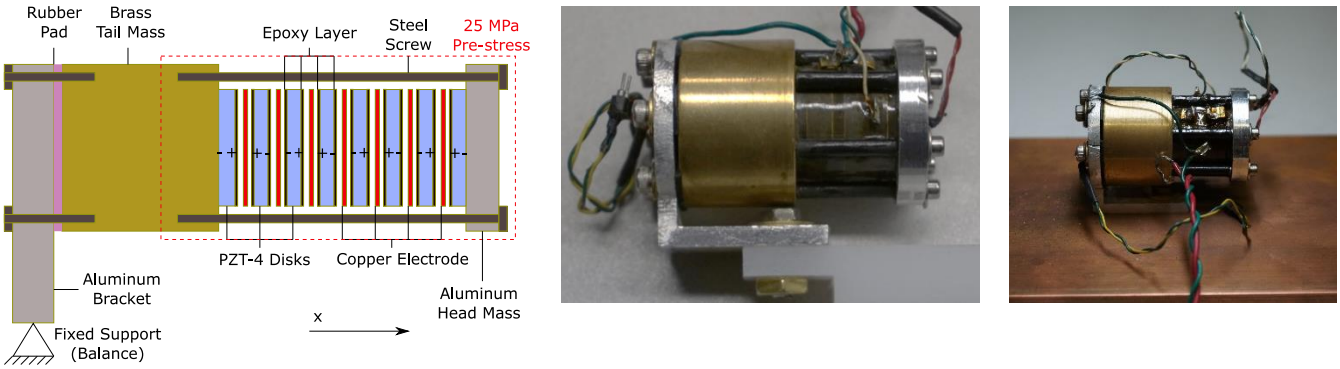

Figure 11: MET Schematics (left), Woodward's MET (middle), TUD MET(right)

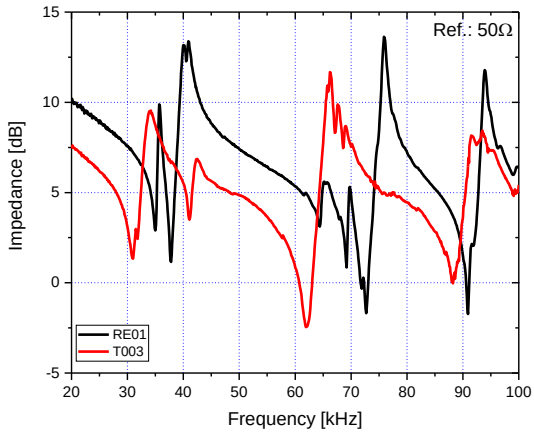

Figure 12: Impedance Spectra Comparison of Woodward and TUD MET

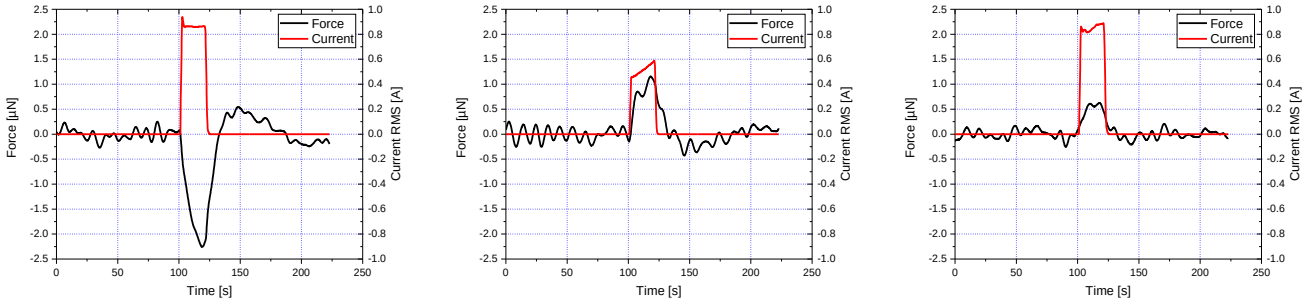

a) 0° b) 180° c) 90°

Figure 13: Average Woodward MET – Single-Mode+Transformer, 140 V, 31 kHz

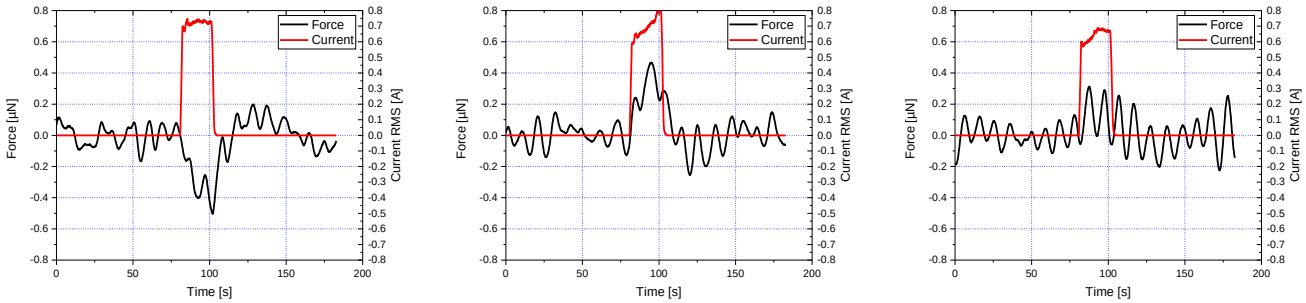

a) 0° b) 180° c) 90°

Figure 14: Average Woodward MET – Single-Mode, 37V, 31 kHz

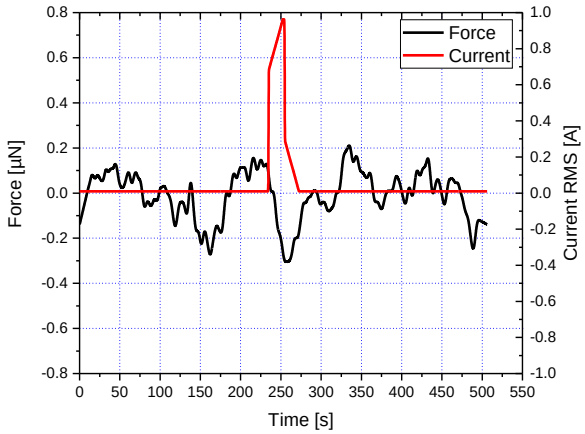

Figure 15: Average Woodward MET – 0°, Sine, Bridge-Mode, 180 V, 31 kHz, Heat Sink

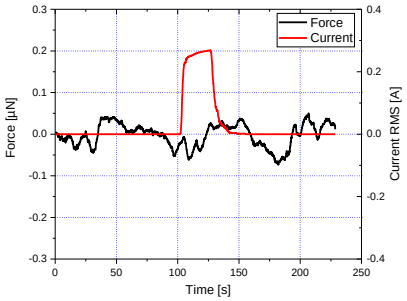

a) 0°

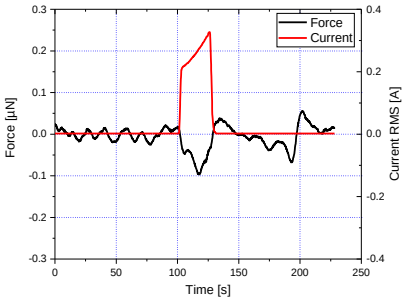

b) 180°

Figure 16: Average TUD MET – Sine, Bridge-Mode, 180V, 36 kHz

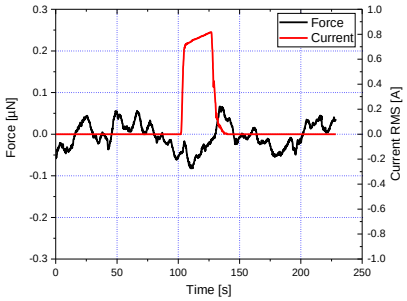

Figure 17: Average TUD MET – 0°, Sine, Bridge-Mode, 180V, 72 kHz

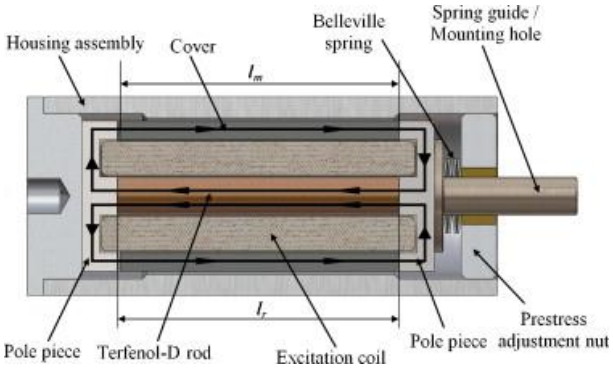

Figure 18: Transducer – CU18A by Etrema (left), Cross-Section of a Magnetostrictive Transducer (right) [13]

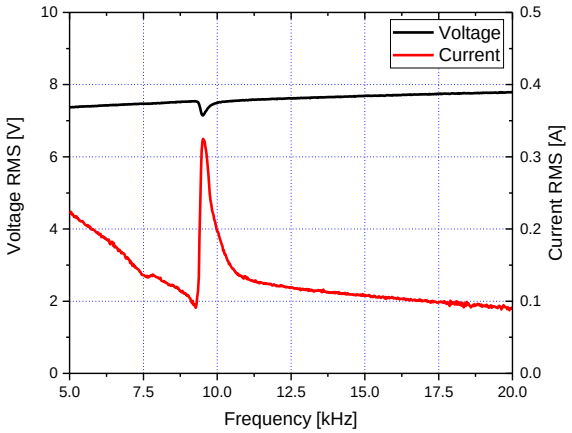

Figure 19: Current and Voltage Spectrum of CU18A

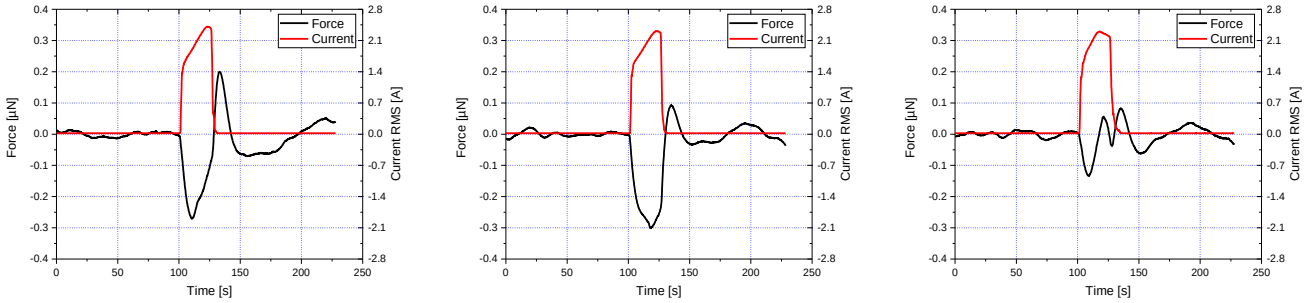

a) 0° b) 180° c) 90°

Figure 20: Average CU18A – Sine, 75 V, 9.6 kHz

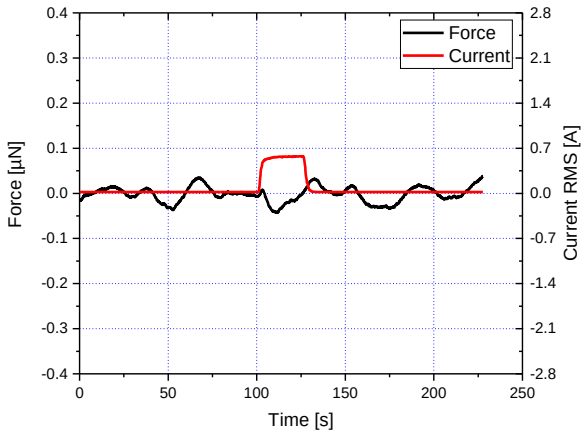

Figure 21: Average CU18A – Mixed 0°

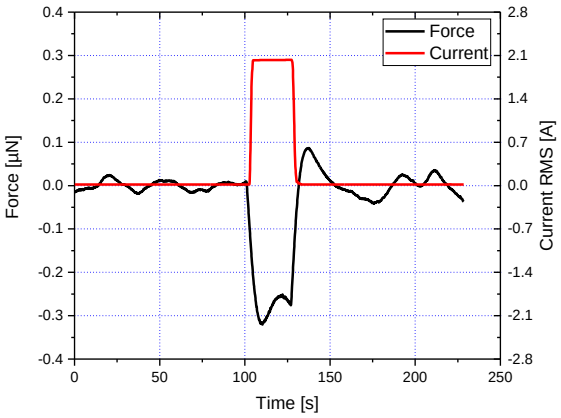

Figure 22: Resistor Setup on Copper Plate (left), Average Resistor – 0°, Sine, 75 V, 9.6 kHz

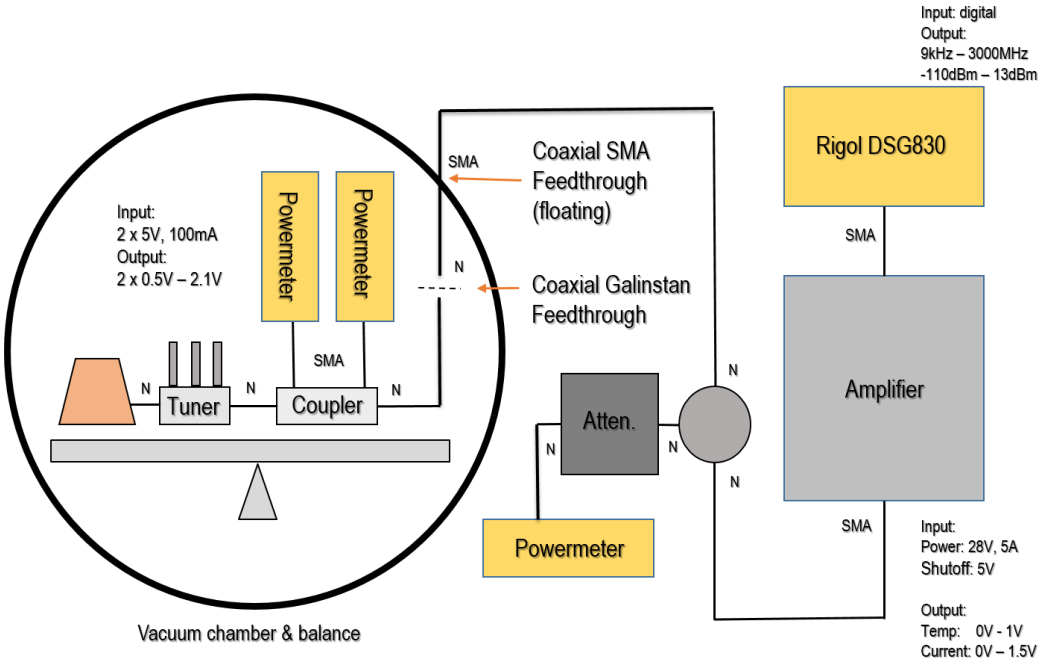

Figure 23: EMDrive Setup

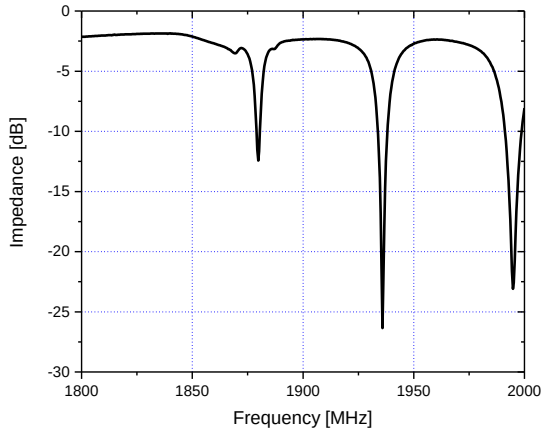

Figure 24: EMDrive Spectrum

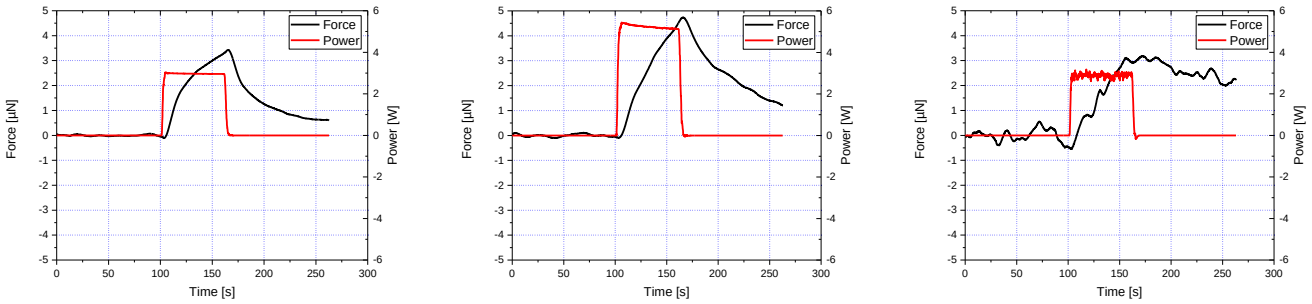

a) HDPE on Flat End-Caps @1933 MHz

b) Flat End-Caps @1920 MHz

c) Spherical End-Caps @2576 MHz

Figure 25: EMDrive Measurements at 0° with Sector 1 Drift Removed